Carbohydrate Polymers 94 (2013) 782–790

Contents lists available at SciVerse ScienceDirect

Carbohydrate Polymers

journal homepage: www.elsevier.com/locate/carbpol

Suspensions of vacuum-freeze dried starch nanoparticles: Influence of NaCl on their rheological properties

Ai-min Shi[a,1], Li-jun Wang[b,1], Dong Li[a,*], Benu Adhikari[c]

[a] College of Engineering, China Agricultural University, P.O. Box 50, 17 Qinghua Donglu, Beijing 100083, China
[b] College of Food Science and Nutritional Engineering, China Agricultural University, Beijing, China
[c] School of Health Sciences, University of Ballarat, VIC 3353, Australia

ARTICLE INFO

Article history:
Received 19 September 2012
Received in revised form 31 January 2013
Accepted 6 February 2013
Available online 14 February 2013

Keywords:
Rheological properties
Starch nanoparticles
Vacuum freeze drying
NaCl
Suspension

ABSTRACT

The effect of addition of NaCl on rheological properties of suspensions containing vacuum freeze dried starch nanoparticles was studied. These starch nanoparticles were produced through high pressure homogenization and emulsion cross-linking technique. Rheological properties such as continuous shear viscosity, storage and loss moduli and creep-recovery were measured. The presence of NaCl at concentration (5–15%, w/v) increased viscosity marginally ($p > 0.05$) while at 20% (w/v) it significantly ($p < 0.05$) increased viscosity. The presence of NaCl enhanced heat stability and weakened gelling capacity of suspensions. NaCl concentration below 15% (w/v) marginally ($p > 0.05$) increased the storage and loss moduli of suspensions. At 20% (w/v), NaCl increased both moduli significantly ($p < 0.05$) within frequency range tested (0.1–10 rad/s). Creep-recovery behavior was affected by NaCl and recovery rate was the highest (98.6%) at 20% (w/v) NaCl. The Cross, Power Law and Burgers' models followed experimental shear viscosity, storage and loss moduli and creep-recovery data reasonably well ($R^2 > 0.94$).

1. Introduction

Suspension containing small particles is a kinetically stable system. Such suspensions are commonly found in nature and in several applied fields such as food, chemical and pharmaceutical industries (Chung, Degner, & McClements, 2012; Deng et al., 2009; Katiyar, Singh, Shukla, & Nandi, 2012; Lee, Choi, Li, Decker, & McClements, 2011). The size of the particles influences the properties and stability of both naturally occurring and artificially created suspensions, especially when the particle size is less than 10 μm (Cheng et al., 2011; Dendukuri & Doyle, 2009; Yin, Xia, Xiang, Qiao, & Zhao, 2009). When the size of the particles is under 1 μm (1000 nm), the suspension can exhibit unique nanometric size effects such as specific surface area and specific mechanical property (Srivastava, Shin, & Archer, 2012; Yin et al., 2009).

Starch nanoparticles (particle size 1–1000 nm) comprising starch molecules and various cross-linkers are new class of small particles (Le Corre, Bras, & Dufresne, 2010). These starch nanoparticles have drawn considerable research interests due to their potential use in high value pharmaceutical and medical industries (Jain, Khar, Ahmed, & Diwan, 2008; Simi & Emilia Abraham, 2007). The preparation, drying, structure analysis and the evaluation of functional performance of starch nanoparticles have drawn considerable research interests because of their potential application as drug carriers (Chakraborty, Sahoo, Teraoka, Miller, & Gross, 2005; Santander-Ortega et al., 2010; Tian & Xu, 2011).

When starch nanoparticles are used for encapsulation and release of therapeutic drugs, they have to be dispersed first into aqueous or other medium to form suspensions. In order to investigate the interaction between the drug and starch nanoparticle, it is necessary to have priori knowledge of interaction occurring amongst the starch nanoparticles. It has been reported that the interactions amongst small particles not only affect the hydrodynamic structure of single particles but also affect the characteristics of the suspending fluid (Lin, Huang, Chang, Anderson, & Yu, 2011; Liu, Wu, Chen, & Chang, 2009).

Rheological methods can be used to quantify the effect of alteration in the characteristics of single particles or particle–particle interaction as well as to quantify the characteristics of the suspending medium (Mewis & Wagner, 2009). The rheological properties such as viscoelasticity can provide useful information during shearing, heating and pressurizing which are common in real-life applications (Tabilo-Munizaga & Barbosa-Cánovas, 2005).

Similarly, the ionic strength of a suspension is another factor which can affect the characteristics of an individual particle in the suspension as well as the properties of suspension (Carneiro-da-Cunha, Cerqueira, Souza, Teixeira, & Vicente, 2011; Chiotelli,

* Corresponding author. Tel.: +86 10 62737351; fax: +86 10 62737351.
E-mail address: dongli@cau.edu.cn (D. Li).
[1] These authors contributed equally to this work.

0144-8617/$ – see front matter © 2013 Elsevier Ltd. All rights reserved.
http://dx.doi.org/10.1016/j.carbpol.2013.02.004

Nomenclature

c	consistency (s)
E_K	modulus of the Kelvin spring (Pa)
E_M	modulus of the Maxwell spring (Pa)
G'	storage modulus (Pa)
G''	loss modulus (Pa)
K	consistency index (Pa s^n)
K'	index (Pa s^n)
K''	index (Pa s^n)
m	flow behavior index (dimensionless)
n'	frequency exponent (dimensionless)
n''	frequency exponent (dimensionless)
R^2	correlation coefficient (dimensionless)
T	absolute temperature (K)
τ	retardation time (s)
τ_2	relaxation time (s)
t	loading time (s)
η_M	viscosity of the Maxwell dashpot (Pa s)
η_K	viscosity of the Maxwell spring dashpot (Pa s)
ω	angle frequency (rad/s)
δ	loss angle (°)
$\dot{\gamma}$	shear rate (s^{-1})
η	apparent viscosity (Pa s)
η_0	viscosity at zero shear rate (Pa s)
η_∞	viscosity at infinite shear rate (Pa s)
ε	strain of suspension (dimensionless)
σ_0	constantly applied compressive stress (Pa)

Pilosio, & Le Meste, 2002). The ionic strength of a suspension can affect the interactions amongst the starch nanoparticles and ultimately affect the rheological properties of the suspension. In this context, there are some publications dealing with the effect of ionic strength on the rheological properties of suspension containing micron size particles from starch and gelatin (Marcotte, Taherian, Trigui, & Ramaswamy, 2001; Wittmar, Ruiz-Abad, & Ulbricht, 2012). These studies have shown that the presence of salts (including NaCl) affects the viscosity, storage and loss moduli and gelatination properties quite significantly. The effect of high ionic strength (produced through the addition of NaCl) on the rheological properties of suspensions containing nanoparticles has been studied. Amiri, Øye, and Sjöblom (2009) and Nasser and James (2009) investigated the effect of salt concentration on the viscoelastic characteristics of suspension containing particles such as silica and kaolinite. These authors also studied the interactions between particles and electrolyte and the consequent manifestation of these interactions on the viscoelastic parameters and thixotropy of the suspension. Besides, the interaction between ionic and counter-ionic components which explains the effect of low molecular weight external electrolyte on the rheological behavior of suspension or gel has also drawn greater attention. Chiotelli et al. (2002) reported that the presence of NaCl introduces complex effect on gelatinization of starch because of NaCl–water and NaCl–starch interactions.

In our recent study we reported the effect of different drying methods on the physical structure and rehydration characteristics of starch nanoparticles. We also investigated the effect of NaCl on the rheological properties of suspension containing spray dried starch nanoparticles (Shi, Li, Wang, & Adhikari, 2012a). As vacuum freeze drying is being increasingly used in drying of high value food and pharmaceutical products we also produced starch nanoparticles by using vacuum freeze drying (Shi, Wang, Li, & Adhikari, 2012). However, the effect of NaCl on the suspension containing vacuum freeze dried starch nanoparticles has not been studied.

In this context, the aim of this manuscript was to investigate the effect of addition of NaCl (in varying concentration) on the rheological properties of suspensions containing vacuum freeze dried starch nanoparticles. In addition, the modeling of continuous shear viscosity data has been carried out using the Cross model. The modeling of the frequency dependence of elastic and loss moduli data has been carried out using Power Law model. Similarly, the experimental creep recovery *versus* time data of the suspensions has been modeled using Burger's model.

2. Experimental

2.1. Materials

Soluble starch (biological reagent) was produced from potato starch through acid-treatment and was purchased from Beijing Aoboxing Biological Technique Company (Beijing, China). Sodium chloride (NaCl), sodium hydroxide, cyclohexane, acetone and acetic acid were analytical grade reagents and were purchased from Beijing Chemical Company (Beijing, China). Polysorbate 80 (Tween-80, food grade) and sorbitan monooleate (Span-80, food grade) were purchased from Tianjing Fuchen Chemical Company (Tianjing, China). Sodium trimetaphosphate (STMP) was analytical grade reagent and obtained from Tianjing Dengfeng Chemical Company (Tianjing, China). Deionized water was used throughout the work.

2.2. Preparation of starch nanoparticles

The starch nanoparticles were produced according to the method reported in pervious paper (Shi, Li, Wang, Li, & Adhikari, 2011). This method adopted the emulsion cross-linking technology using a high pressure homogenizer. Briefly, 8 g of soluble starch was firstly added to 30 g NaOH (5%, w/v) solution. In another bottle, 2 g of sodium trimetaphosphate (STMP) was added to 20 g of NaCl (7.5%) solution. These two solutions were quickly mixed and were immediately poured into 150 ml cyclohexane containing emulsifiers (1.44 g Tween-80 and 7.56 g Span-80) to produce w/o emulsion. The emulsion was produced by using a high speed rotor-stator homogenizer (IKA® T25 digital, Staufen, Germany) maintaining at 10,000 rpm for 2 min. Subsequently, the nanoemulsion was prepared using high pressure homogenizer at 10 MPa using 2 cycles or passes. The starch nanoparticles were obtained after 12 h long cross-linking and solidification process. The cross linking temperature and stirring speed were 25 °C and 250 rpm. Magnetic stirrer was used for this slow stirring. The optical images of the starch nanoparticles in w/o emulsion were taken using a 400× optical microscope coupled with a digital camera (Olympus® CX31, Olympus Instruments, Tokyo, Japan) and the particle size was analyzed by a laser particle size analyzer (NanoZS-90, Malvern, England) (Shi et al., 2011).

After demulsification with 10% glacial acetic acid and twice washing with acetone, starch nanoparticles from 40 ml mini-emulsion were dissolved into 100 ml deionized water. This suspension was stirred for 1 h to ascertain that all the starch nanoparticles were completely dispersed. Finally, this suspension was transferred to drying dish (0.1 $m^2 \times 3$ cm) for vacuum freeze drying.

2.3. Vacuum freeze drying of starch nanoparticles

The vacuum freeze drying of starch nanoparticles was reported in detail in our previous research (Shi, Wang, et al., 2012). Briefly, the sample dishes (0.1$m^2 \times 0.03$ m) containing the suspension of starch nanoparticles (0.1$m^2 \times 0.01$ m) were placed in the cold trap (−60 °C) of the vacuum freeze dryer (LGJ-18, Sihuan, China) for 5 h to ensure complete freezing of the sample. Subsequently, the frozen

samples were placed in drying chamber and then the chamber was evacuated (<100 Pa). The temperature of frozen sample was varied from −30 °C to 45 °C step by step in the 28 h-long drying period (1 h each at −30 °C, −25 °C, −20 °C, −15 °C, −10 °C, −5 °C; 2 h each at 0 °C, 5 °C, 10 °C, 15 °C, 20 °C, 25 °C, 30 °C, 35 °C, 40 °C and finally 4 h at 45 °C).

The vacuum freeze dried starch nanoparticles were stored in desiccators under desired storage temperature and humidity (25 °C and 10% RH). A scanning electron microscope (S-3400N, Hitachi, Japan) was used to take microphotographs of the starch nanoparticles.

2.4. Preparation of starch nanoparticle suspensions for rheological tests

Five 6% (w/v) starch nanoparticle suspensions containing as 0% salt (0 g NaCl and 0.6 g starch nanoparticles in 10 ml DI water), 5% (w/v) salt (0.5 g NaCl + 0.6 g starch nanoparticles in 10 ml DI water), 10% (w/v) salt (1 g NaCl + 0.6 g starch nanoparticles in 10 ml DI water), 15% (w/v) salt (1.5 g NaCl + 0.6 g starch nanoparticles in 10 ml DI water), 20% (w/v) salt (2 g NaCl + 0.6 g starch nanoparticles in 10 ml DI water) were prepared using a magnetic stirrer for 30 min at 25 °C for rheological tests.

2.5. Rheological tests

As a follow-up study on the effect of NaCl on the suspension containing starch nanoparticle, we adopted the same rheological tests for the suspensions containing vacuum freeze dried starch nanoparticles as we had in our previous research (Shi et al., 2012a). Specifically, four types of rheological tests were performed in the absence and presence of NaCl: (1) to obtain apparent viscosity *versus* shear rate for the suspension, continuous shear measurements were carried out; (2) to establish a relationship between viscoelastic modulus and temperature of the suspension, temperature sweep tests were employed; (3) to study the relationship between the viscoelastic modulus and frequency of the suspension, frequency sweep measurements were conducted; and (4) to find out the creep behavior of suspension, the creep-recovery tests were carried out. The rheological tests were performed using a AR2000ex rheometer (TA Instruments Ltd., New Castle, DE). An equilibration time of 2 min was maintained before each measurement.

For all rheological tests described as follows, 0.5 ml of the suspension (explained in Section 2.4) was added on the Peltier plate (aluminum, 40 mm diameter, 1 mm gap) and then upper parallel plate was moved down to provide the 1 mm gap. After removing the excess suspension and applying silica oil on the edge of the plate, the tests were commenced according to the following parameters.

2.5.1. Continuous shear tests

The continuous shear tests were performed at 25 °C over the shear rate range of 0.1–100 s^{-1} to measure the apparent viscosity.

In addition, we modeled the flow curves or experimental viscosity *versus* shear rate data (Susan-Resiga, Bica, & Vékás, 2010) using Cross equation (Eq. (1)) by non-linear regression feature of SPSS 13.0 software (SPSS Inc., Chicago, USA).

$$\eta = \eta_\infty + \frac{\eta_0 - \eta_\infty}{1 + (c\dot{\gamma})^m} \quad (1)$$

where η is the apparent viscosity (Pa s), η_∞ is the viscosity at infinite shear rate (Pa s), η_0 is the viscosity at zero shear rate (Pa s), c is the consistency (s), $\dot{\gamma}$ is the shear rate (s^{-1}), and m is the flow behavior index (dimensionless) (Corcione, Cavallo, Pesce, Greco, & Maffezzoli, 2011).

2.5.2. Temperature sweep tests

The temperature sweep measurements were carried out using a frequency of 1 Hz and oscillating stress of 0.7958 Pa. The test temperature was increased from 25 °C to 90 °C at a heating rate of 2 °C/min and then decreased to 25 °C at the same cooling rate.

2.5.3. Frequency sweep tests

The frequency sweep tests were performed at 25 °C over the angular frequency range of 0.1–10 rad/s. The oscillating stress for the frequency sweep measurements was selected to be 0.7958 Pa based on the strain sweep results (data not shown) in order to confine these tests within the linear viscoelastic region of all samples.

Power Law models based on Eqs. (2) and (3) were also used to analyze the frequency dependence of G' and G'' data presented in Fig. 4 by non-linear regression feature of SPSS 13.0 software (SPSS Inc., Chicago, USA) (Wang, Wang, Li, Xue, & Mao, 2009).

$$G' = K' \cdot \omega^{n'} \quad (2)$$

$$G'' = K'' \cdot \omega^{n''} \quad (3)$$

where K' and K'' are Power Law constants and reflect the elastic and viscous properties, respectively. n' and n'' are referred to the frequency exponents and ω is the angular frequency (rad/s).

2.5.4. Creep-recovery tests

Creep-recovery experiments were carried out using a shear stress of 7.958 mPa at 25 °C. The variation of shear strain in response to the applied shear stress was measured over a period of 5 min. The shear stress was subsequently removed, and the changes in strain were recorded for a further period of 5 min.

Burger's model, which is comprised of both Maxwell and Kelvin models arranged in series (Jia, Peng, Gong, & Zhang, 2011) and is represented by Eq. (4), was used to predict the creep recovery behavior of these suspensions.

$$\varepsilon = \frac{\sigma_0}{E_M} + \frac{\sigma_0}{E_K}(1 - e^{-t/\tau}) + \frac{\sigma_0}{\eta_M} \cdot t \quad (4)$$

where ε represents the strain (%) of suspension, t represents the time (s) after loading, E_M and η_M are the modulus (Pa) and viscosity (Pa s) of Maxwell spring and dashpot, respectively. Similarly, E_K and η_K are the modulus (Pa) and viscosity (Pa s) of the Kelvin spring and dashpot, respectively. Similarly, $\tau = \eta_K/E_k$ is the time taken to recover 63.2% or $(1 - e^{-1})$ of the total deformation in the Kelvin unit. The parameters E_M, E_K, η_M, and τ were obtained from fitting the experimental data to Eq. (4).

2.6. Statistical analysis

All of these rheological measurements were carried out in triplicate. The experimental rheological data were obtained directly from the TA Rheology Advantage Data Analysis software V 5.4.7 (TA Instruments Ltd., Crawley, UK). The average of three experimental runs was reported as the measured value along with the standard deviation.

Duncan's multiple comparison method was used to determine the significant/insignificant effect using the SAS software (SAS Institute Inc., Cary, NC, USA) at a confidence level of 0.95. Meanwhile, t-test was used to make sure all the residuals followed the normal distribution.

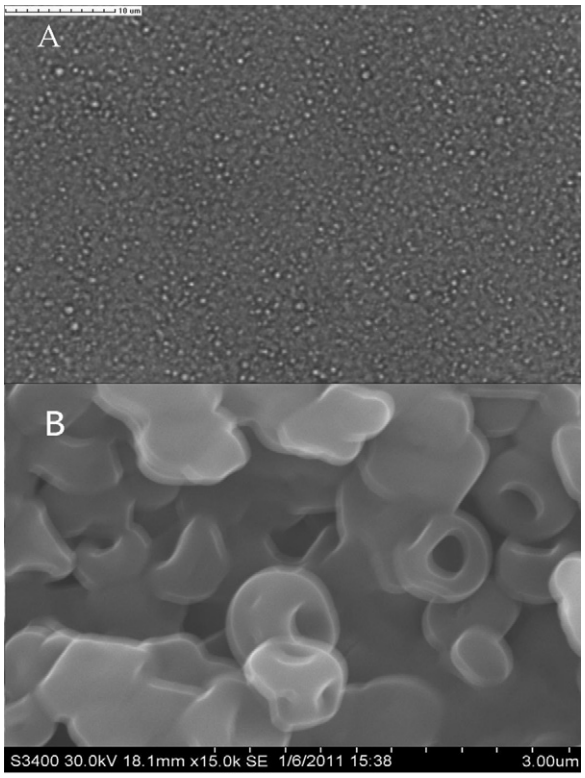

Fig. 1. The morphology of starch nanoparticles. (A) Optical image of starch nanoparticles in w/o emulsion; (B) SEM micrograph of vacuum freeze dried starch nanoparticles.

3. Results and discussion

3.1. Morphology and particle size of the dried starch nanoparticles

Starch nanoparticles were prepared by the water-in-oil (w/o) mini-emulsion crosslinking technique using high pressure homogenizer. After solidification/stabilization via crosslinking reaction (Eq. (I)), starch nanoparticles were formed in w/o mini-emulsions (Fig. 1(A)). These starch nanoparticles were uniform and their mean particle size varied between 300 and 500 nm (Shi, Wang, et al., 2012).

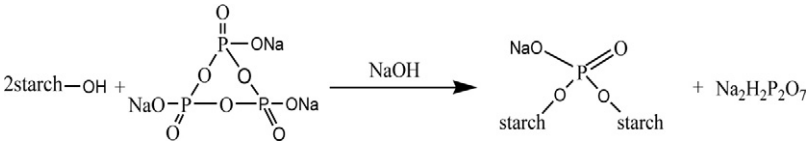

(I)

The morphology of the starch nanoparticles using SEM is presented in Fig. 1(B). The mean particle size of the starch nanoparticles obtained by SEM is around 600–900 nm which is higher than the mean particle size when they were still in w/o emulsion. As these nanoparticles were dispersed in water before vacuum-freeze drying, it appears that some swelling of these starch nanoparticles occurred prior to the drying which increased the mean particle size. Some of these starch nanoparticles appeared to be hollow which can be attributed to the sublimation of ice or evaporation of water.

3.2. Continuous shear behavior

The steady shear flow curves of 6% (w/v) suspension of vacuum freeze dried starch nanoparticles with varying NaCl concentration are presented in Fig. 2 and the results are quite different from our previous research on the suspension containing spray dried starch nanoparticles (Shi et al., 2012a).

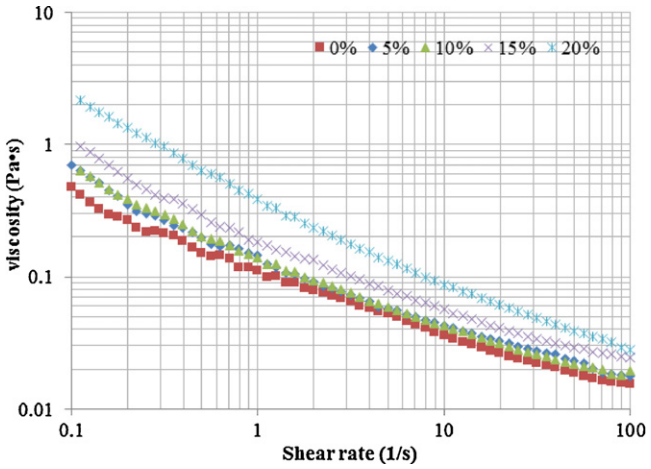

Fig. 2. Effect of the NaCl concentration (w/v) on the apparent viscosity of 6% (w/v) suspension of vacuum freeze dried starch nanoparticles.

Specifically, the additional of NaCl increases the viscosity of the suspension within the shear rate range (0.1–100 s^{-1}) tested. The suspension without NaCl showed the lowest viscosity while suspension with 20% (w/v) of NaCl had the highest viscosity at any corresponding shear rates. As many of these starch nanoparticles are hollow and have appreciable porosity created because of vacuum freeze drying, they are easy to re-disperse in water and considerable swelling or expansion of these particles is expected when dispersed in water. Furthermore, the collision amongst starch nanoparticles is common and easily affected by the presence of salt because of the compression of electric double layer (EDL) and the decrease in the Debye's length of starch nanoparticles. With the increase in salt concentration, these effects exert more influences on the viscosity of suspension. The shear viscosity is affected by the collision between starch nanoparticles and the variation in the shear viscosity is one of the manifestations of the collision amongst these particles in aqueous medium.

The shear stress *versus* shear rate data of the aqueous NaCl solutions within the concentration range (at 20 °C) are known to vary linearly and the Newtonian viscosity values of the solutions have reported to vary 1.076×10^{-3} Pa s (at 5%) to 1.418×10^{-3} Pa s (at 20%) (Kestin, Khalifa, & Correia, 1981). This means that even the lowest viscosity value of the starch nanoparticle suspensions is 100 times higher than the viscosity values of the salt solutions. These low viscosity values of the salt solutions suggest that the effect of the salt is not because of bulk mixing rule in viscosity rather it is the effect of ions on electric double layer.

We can also observe from Fig. 2 that all the aqueous suspensions of the starch nanoparticles with or without NaCl exhibit shear thinning behavior within the shear rate range tested (0.1–100 s^{-1}). The continuous shearing process can accelerate the re-dispersion of starch nanoparticles into the suspension forming uniform and orderly organization amongst the starch nanoparticles. The shearing process affects the collision which finally gets reflected into or gets manifested in the magnitude and the variation of viscosity with shear rate. Meanwhile, the apparent viscosity data shown in

Table 1
Cross modeling parameters of apparent viscosity of 6% (w/v) vacuum freeze dried starch nanoparticles suspension containing different NaCl concentration (w/v).*

NaCl concentration (%, w/v)	η_0 (Pa s)	η_∞ (Pa s)	c (s)	m	R^2
0	43.851 ± 2.326[a]	0.018 ± 0.003[a]	9823.127 ± 176.807[a]	0.677 ± 0.038[a]	0.990
5	291.948 ± 33.621[b]	0.028 ± 0.003[a]	14,967.596 ± 120.572[b]	0.837 ± 0.038[b]	0.993
10	103.113 ± 31.781[c]	0.021 ± 0.002[a]	8551.089 ± 134.950[c]	0.753 ± 0.023[b]	0.997
15	394.003 ± 30.094[d]	0.034 ± 0.004[a]	12,371.702 ± 112.223[d]	0.841 ± 0.029[b]	0.996
20	354.168 ± 19.785[d]	0.031 ± 0.003[a]	4820.501 ± 163.467[e]	0.815 ± 0.008[b]	0.999

* Values represent the mean ± standard deviation of triplicate tests.
Values in a column with different superscripts were significantly different ($p < 0.05$).

this figure also suggest that the increase in the NaCl concentration from 5% to 20% does not alter the shear thinning trend. When the shear rate reaches 100 s^{-1}, the viscosity values of suspensions with and without NaCl are very close to each other. This explains the fact that the effect of shear rate on the suspension viscosity is more dominant than the effect of NaCl concentration.

The parameters obtained by fitting the Cross model to experimental data are presented in Table 1. This table shows very strange trend for the viscosity values at zero shear rate. Basically, adding of NaCl can significantly ($p < 0.05$) enhance this limiting viscosity of suspension at zero shear rate. However, the viscosity values at infinite shear rate at different NaCl concentrations are not significantly different ($p > 0.05$). The viscosity values at zero shear rate at different NaCl concentrations firstly increased from 43.851 Pa s to 291.948 Pa s when the NaCl concentration increased from 0% to 5%. Subsequently, when the NaCl concentration increased from 5% to 10%, the viscosity reduced (instead of increasing) from 291.948 Pa s to 103.113 Pa s. For instance, the viscosity values were 394.003 Pa s at 15% NaCl and 354.168 Pa s at 20% NaCl. However, the viscosity values at infinite shear rate were not statistically different and there was no clear increasing or decreasing trend when the NaCl concentration was over 5%. The consistency parameter (c value) of the suspensions also did not show any consistent change or variation with the increase in the NaCl concentration. The flow behavior index (m) values of suspensions (Table 1) indicate that the increase in the concentration of salt from 5% to 20% does not significantly ($p > 0.05$) affect the shear thinning behavior of these suspensions. However, the m value of the starch nanoparticles-only suspension is remarkably ($p < 0.05$) lower than the m values of the suspensions containing NaCl.

3.3. Effect of temperature on dynamic rheological properties

The variation of storage modulus (G'), loss modulus (G''), and loss angle (δ) as a function of temperature is presented in Fig. 3. The figures with uppercase letters represent the period in which the temperature is increased (25–90 °C) while the figures with lowercase letters represent the period in which the temperature is decreased (90–25 °C). In both the heating and cooling processes, Fig. 3(A) and (a), the storage modulus of suspension containing only the starch nanoparticles shows large variation with the change in temperature. At the same test conditions, the suspensions containing NaCl show only subtle variation in the storage modulus. This might be due to the fact that NaCl can affect the electric double layers of starch nanoparticles and Debye's length, and alter the suspension density. The presence of salt might facilitate the interaction amongst starch nanoparticles which can result into suspensions with better thermal stability.

It is interesting to note that the storage modulus of the starch-only nanoparticle suspensions increased quite remarkably above 70 °C which can be explained based on the fact that heating might have caused expansion and disruption of inter and intra molecular hydrogen bonds in starch nanoparticles and increased the starch–water hydrogen bonds. The increase in the temperature of the suspension facilitates the swelling of starch nanoparticles (Chung, Min, Kim, & Lim, 2007). This is the reason why the storage modulus of suspension containing only the starch nanoparticles decreased first and then increased later when it was heated from 25 °C to 90 °C. When NaCl was added into these suspensions, the strong ionic environment provided a buffering environment around the starch nanoparticles allowing the suspensions to resist the effect of temperature during heating and cooling (Batrd-Parker, Boothroyd, & Jones, 1970). This kind of buffering effect is enhanced when the concentration of NaCl is increased.

It can be seen from Fig. 3(B) and (a) that the trend of variation in the loss modulus (G'') of all these NaCl containing suspensions at all the NaCl concentration levels is similar within the entire temperature range. Specifically, when the temperature of suspensions increased from 25 °C to 90 °C, the loss modulus decreased first before increasing. During the cooling period (90–25 °C), the loss modulus recovered to the value which was close to the initial one. The loss modulus decreased first when the NaCl concentration increased from 0% to 5%. Subsequently, it increased when the NaCl concentration increased from 10% to 20%. When small amount of NaCl is present in aqueous suspension of starch nanoparticles, the presence of NaCl causes the compression of electrical double layer (EDL). As a consequence, when the concentration of NaCl increases, the viscosity which can be calculated from loss modulus (Barnes, Hutton, & Walter, 1989) decreases because of the weakening of interactions amongst starch nanoparticles. When excess amount of NaCl is present in the suspension, it induces coagulation which explains the increase in the loss modulus (viscosity) (Xin et al., 2007).

The value of loss angle (δ) is commonly used to explain the gelling properties of suspension containing macromolecules. During the heating and cooling cycles, the suspension, which did not contain NaCl, showed remarkable decrease in loss angle which can be attributed to the gelling of starch nanoparticles (Fig. 3(C) and (c)). However, such a high degree of change in the loss angle was not observed in suspensions containing NaCl. These results suggest that the presence of NaCl affects the internal structure of suspension during heating and cooling and ultimately affects the storage modulus, loss modulus and loss angle.

3.4. The frequency dependence of dynamic rheological properties

Fig. 4 presents the variation of storage modulus (G'), loss modulus (G'') and loss angle (δ) as a function of frequency (0.1–10 rad/s) and NaCl concentration (0–20%, w/v) in the suspension containing 6% (w/v) starch nanoparticles. As can be seen from this figure, the loss modulus (G'') values of all the suspensions are higher than the corresponding storage modulus (G') values over the entire frequency range (0.1–10 rad/s). This observation suggests that the viscous behavior is dominant over elastic behavior in starch nanoparticle suspensions (Lu, 2007), no matter how much NaCl is added within the NaCl concentration tested (20%, w/v, NaCl). In all these suspensions, the storage and loss moduli increased and loss angle decreased when the angular frequency increased. This might

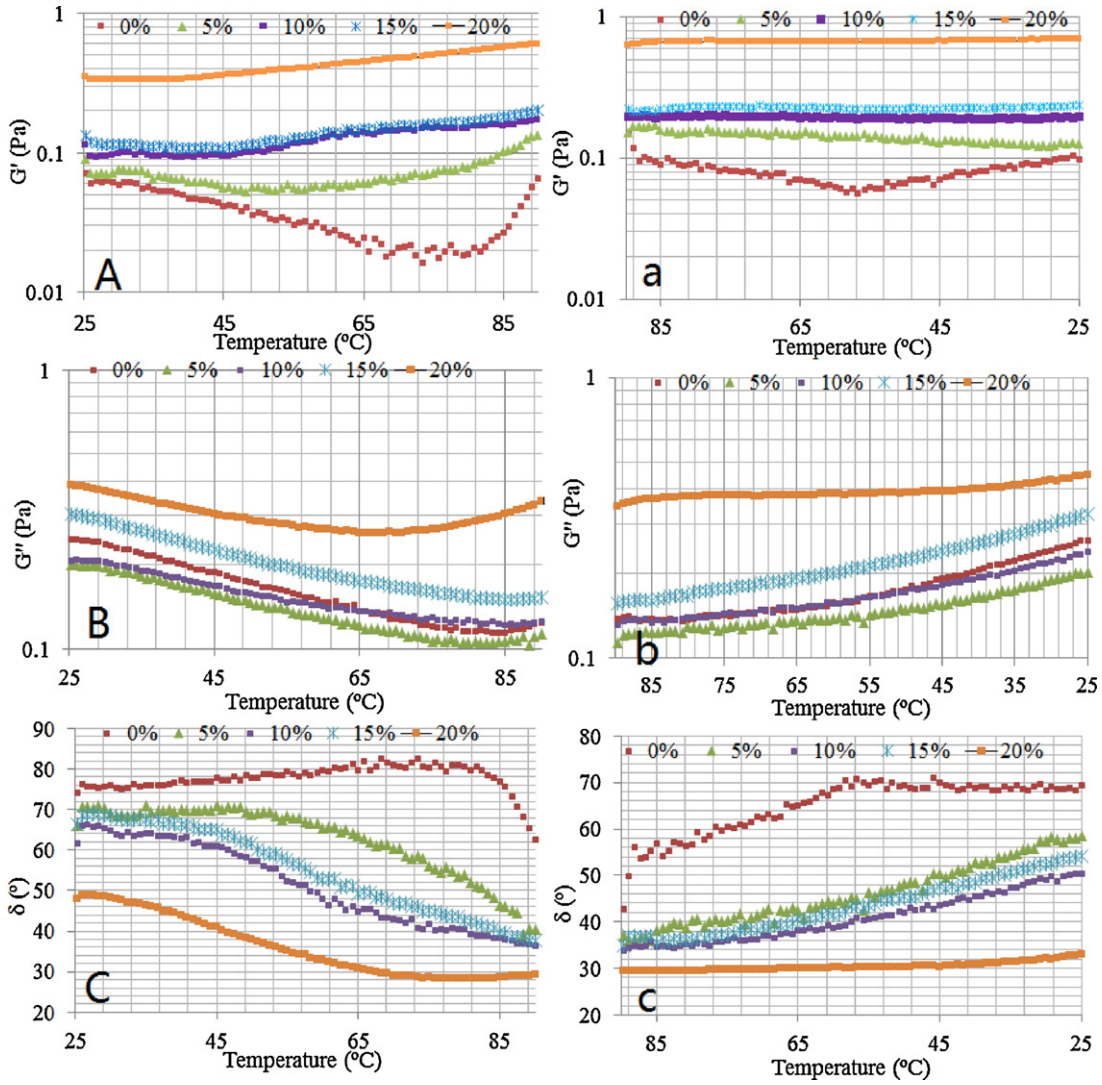

Fig. 3. The variation of elastic modulus (G'), loss modulus (G'') and loss angle (δ) of 6% (w/v) starch nanoparticle suspensions (containing 0–20% (w/v) NaCl) as a function of temperature. (A, B and C) Temperature-rise period; (a, b and c) temperature-drop period.

have been resulted from the alteration in the internal structure of suspension under oscillating stress (Li & Huang, 2012).

Another clearly observable feature in this figure is that both the storage and loss moduli of the suspension increased significantly ($p < 0.05$) at 20% (w/v) NaCl while suspensions with 0–15% (w/v) of NaCl concentration have very close storage and loss modulus values ($p > 0.05$). The increase in the storage and loss moduli can also be explained based on the fact that the presence of NaCl affects the internal structure of the suspension which was also observed in continuous shear and temperature sweep measurements. At higher oscillating frequencies, the starch nanoparticles have higher probability of colliding amongst each other during the oscillation process. The increase in kinetic energy (due to higher mechanical energy input) finally gets transformed into the increase in both the storage and loss moduli (Lu, 2007). This is the reason why even at high NaCl concentration the starch nanoparticle suspensions show consistently increasing trends both in the storage and loss moduli. The loss angles of these suspensions also follow the above feature and decrease with the increase in the frequency (Fig. 4(C)). This observation suggests that the rate of increase in the storage modulus is higher than the rate of increase in the loss modulus when oscillating frequency is increased. The presence of NaCl can increase both the storage and loss moduli of the suspensions. However, a significant increase in the storage and loss moduli occurred only when the NaCl concentration was 20% (w/v). This is the reason why the loss angle of suspension containing 20% (w/v) NaCl decreased remarkably with increase in frequency while loss angle values of other suspensions at lower NaCl concentrations were close to each other and showed similar decreasing trend with increase in frequency.

As can be seen from Table 2, the regression coefficients are higher than 0.98 and the average absolute error in prediction ranged from 0.19% to 1.18% suggesting that the Power Law model represents the experimental G' and G'' data well. The K'' values of all these suspensions are higher than the K' values. This indicates that the suspensions containing starch nanoparticles display higher viscous effect than elastic effect within the frequency range of 0.1–10 rad/s. The fact that the values of loss angle decreased from 90° to 45° corroborates to the fact that the elastic component is increasing, however, it is not quite dominant. In addition, Table 2 further shows that the K' and K'' values of suspensions containing 0–15% (w/v) of NaCl are very close to each other while both the K' and K'' of suspension containing 20% (w/v) of NaCl increased significantly. It can also be seen from Table 2 that the n' values are higher than the n'' values in all the samples. The variation of n' and n'' with the increase in the NaCl concentration does not seem to follow any particular trend except in the case of suspension containing

Table 2
Power Law parameters of elastic and loss moduli of 6% (w/v) vacuum freeze dried starch nanoparticles suspension containing different NaCl concentration (w/v).*

NaCl concentration (%, w/v)	K' (Pa s^n)	n'	R^2	K'' (Pa s^n)	n''	R^2
0	0.004 ± 0.0003[a]	1.320 ± 0.044[a]	0.980	0.049 ± 0.001[a]	0.871 ± 0.009[a]	0.998
5	0.006 ± 0.001[a]	1.288 ± 0.049[a]	0.982	0.045 ± 0.001[a]	0.808 ± 0.014[a]	0.994
10	0.007 ± 0.001[a]	1.324 ± 0.054[a]	0.980	0.050 ± 0.002[a]	0.783 ± 0.017[a]	0.992
15	0.010 ± 0.001[a]	1.220 ± 0.041[a]	0.985	0.065 ± 0.001[b]	0.817 ± 0.012[a]	0.996
20	0.041 ± 0.002[b]	1.062 ± 0.031[a]	0.988	0.111 ± 0.003[c]	0.671 ± 0.013[b]	0.993

* Values represent the mean ± standard deviation of triplicate tests.
Values in a column with different superscripts were significantly different ($p < 0.05$).

20% (w/v) of NaCl. This may be due to the fact that the frequency sensitivity of suspensions containing vacuum freeze dried starch nanoparticles gets substantially decreased when the concentration of NaCl is high enough (Wang et al., 2009). This observation also suggests that low concentration of NaCl (5–15%, w/v) is unable to alter the interactions amongst starch nanoparticles and structure formed because of these interactions remains intact.

3.5. Creep-recovery behavior of starch nanoparticles suspensions

Fig. 5 presents the creep-recovery behavior of suspension containing vacuum freeze dried starch nanoparticles at various NaCl concentrations. The strain *versus* time data presented in Fig. 5(A) show that the suspension containing 10% (w/v) of NaCl deform the most and suspension containing 20% (w/v) of NaCl deformed the

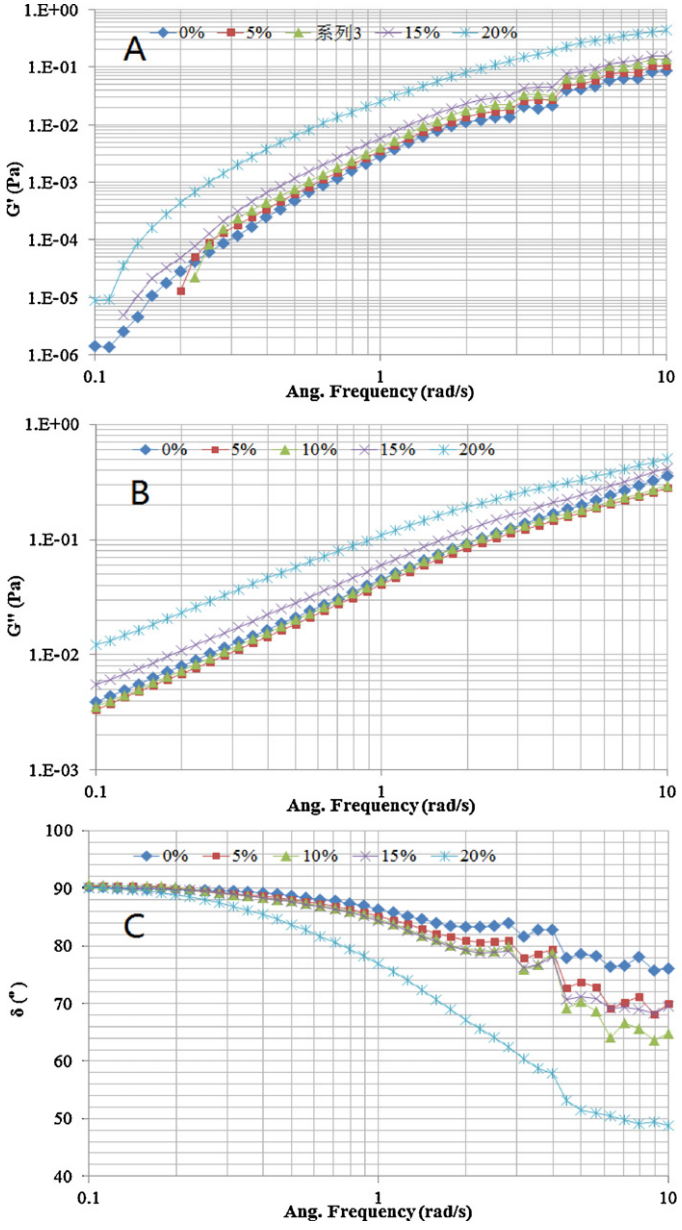

Fig. 4. Frequency dependence of G', G'' and loss angle (δ) in 6% (w/v) vacuum freeze dried starch nanoparticles suspension containing different NaCl concentrations (w/v).

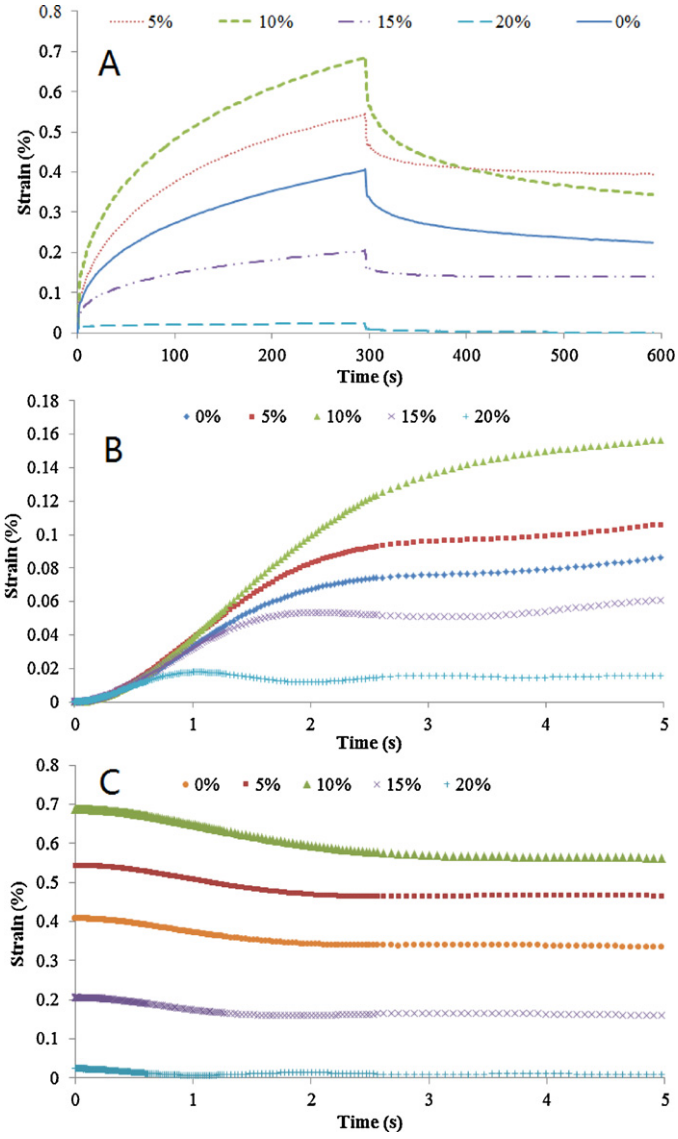

Fig. 5. Creep-recovery behavior of 6% (w/v) vacuum freeze dried starch nanoparticles suspension containing different NaCl concentrations (w/v).

Table 3
Burger's modeling parameters of creep-recovery behavior of 6% (w/v) vacuum freeze dried starch nanoparticles suspension containing different NaCl concentration (w/v).*

NaCl concentration (%, w/v)	E_K (Pa)	τ (s)	η_M (Pa s)	R^2	Recovery (%)
0	0.052 ± 0.001[a]	6.533 ± 0.317[a]	8.043 ± 0.116[a]	0.986	44.5
5	0.037 ± 0.001[b]	8.940 ± 0.318[b]	6.047 ± 0.102[b]	0.984	27.2
10	0.028 ± 0.001[c]	8.685 ± 0.297[b]	5.146 ± 0.084[c]	0.987	49.8
15	0.094 ± 0.001[d]	3.194 ± 0.124[c]	16.172 ± 0.268[d]	0.977	30.8
20	0.483 ± 0.008[e]	0.594 ± 0.020[d]	262.949 ± 12.151[e]	0.945	98.6

* Values represent the mean ± standard deviation of triplicate tests.
Values in a column with different superscripts were significantly different ($p < 0.05$).

least. Fig. 5(B) and (C) shows the expanded view of the first 5 s of the creep section and the recovery section, respectively. In these two figures, the trend described in Fig. 5(A) can also be observed. The strain *versus* time data shown in the panel (B) and (C) of Fig. 5 at a fixed stress (7.958 mPa) suggest that these suspensions of vacuum freeze dried starch nanoparticles are stable within the salt concentrations tested and that the presence of NaCl affects the extent of deformation at the initial stage of creep as well as recovery.

In Eq. (4), the strain can be a constant value (σ_0/E_M) when the time is zero, which means that the suspension will display an instantaneous elastic deformation. However, we did not observe such instantaneous deformation in the ordinate of Fig. 5(B). Hence, we only used the second and third terms in Eq. (4) as shown by Eq. (5).

$$\varepsilon = \frac{\sigma_0}{E_K}(1 - e^{-t/\tau}) + \frac{\sigma_0}{\eta_M} \cdot t \quad (5)$$

Eq. (5) represented the experimental creep recovery *versus* time data reasonably well ($R^2 > 0.94$, average absolute errors 0.71–1.76%) and the parameters obtained in best fit scenario are presented in Table 3. Amongst these suspensions, the suspension containing 10% (w/v) of NaCl shows the lowest E_K and η_M values and the second longest τ value (statistically insignificant with the highest τ value, $p > 0.05$). Interestingly, the starch nanoparticles suspension containing 20% (w/v) of NaCl had the highest E_K and η_M values and the lowest τ value.

The parameter E_K and η_M represent the recovered elastic deformation under steady applied pressure and the viscosity of the suspension, respectively. From the E_K and η_M data of suspension containing 10% (w/v) of NaCl, it can be observed that this suspension has lost substantial amount of energy (due to higher strain) during the ordering process of starch nanoparticles in the initial stage of creep (Fig. 5(B)) while this process is considerably short in suspension containing 20% (w/v) NaCl. On the other hand, the suspension containing 20% (w/v) of NaCl exhibited better recovery behavior (recovery rate) (Table 3) than other suspensions as can be seen from the maximally recovered elastic deformation.

3.6. Comparative analysis with suspensions of spray dried starch nanoparticles

When the results from this study are compared with those presented in our previous research in which the effect of NaCl on the rheological properties of spray dried starch nanoparticles (Shi et al., 2012a) were presented, it can be seen that the presence of NaCl is capable of significantly ($p < 0.05$) affecting the rheological properties of starch nanoparticle suspensions including the continuous shear viscosity, dynamic rheology (variation of elastic and viscous moduli with temperature or frequency) and creep recovery. The comparison also shows that the variation of NaCl concentration in the suspensions only shows marginal ($p > 0.05$) influences on their rheological properties.

Interestingly, the presence of NaCl on the shear viscosity and viscous modulus of suspensions containing spray dried starch nanoparticles and vacuum freeze dried starch nanoparticles exhibited quite opposite trends. For example, as can be seen from Fig. 2, the apparent viscosity of the suspension containing vacuum freeze dried starch nanoparticles increased consistently in the presence of NaCl (in all the salt concentration tested). However, we had found that the presence of salt decreased the shear viscosity of the suspensions containing spray dried nanoparticles in the same shear rate range and at the same salt concentrations (Shi et al., 2012a). These findings indicate that different drying methods such as vacuum freeze drying and spray drying used in producing starch nanoparticles affect the re-dispersion characteristics of the starch nanoparticles in water (Shi, Li, Wang, & Adhikari, 2012b). In addition, the application of different drying methods results into different particle size and shape in starch nanoparticles (Shi, Wang, et al., 2012; Shi, Li, Wang, Zhou, & Adhikari, 2012) and ultimately affects the interaction between these particles.

4. Conclusions

The presence of NaCl up to 15% (w/v) did not increase the viscosity of suspension significantly ($p > 0.05$) while at 20% (w/v) of NaCl the viscosity of the suspension was increased significantly ($p < 0.05$). All these suspensions exhibited shear-thinning behavior and the absence or presence of NaCl and the variation of NaCl concentration did not alter this trend. The viscosity *versus* shear rate data of all the suspensions were found to be well represented by the Cross model ($R^2 > 0.9$, average absolute errors = 0.56–1.11%). The presences of NaCl enhanced the heat stability and weakened the gelling behavior of starch nanoparticle suspensions. The loss modulus values of all the suspensions were higher than their corresponding storage modulus values over the entire frequency range (0.1–10 rad/s). The presence of NaCl concentration (20%, w/v) in the suspension increased the storage modulus and loss moduli values significantly ($p < 0.05$). The addition of NaCl up to 15% (w/v) did not increase the storage and loss moduli of starch nanoparticle suspensions significantly ($p > 0.05$). The experimental storage and loss moduli data were fitted well by the Power Law model ($R^2 > 0.98$, average absolute errors = 0.19–1.18%). In the creep-recovery test, the containing 10% (w/v) of NaCl deformed the most and suspension containing 20% (w/v) NaCl deformed the least while the Burger's modeling predicted the creep recovery data reasonably well ($R^2 > 0.94$, average absolute errors = 0.71–1.76%). The parametric analysis of Burger's model showed that the suspension containing 10% (w/v) NaCl recovered the least while the suspension containing 20% (w/v) of NaCl recovered the most.

The effect of NaCl on the shear viscosity of suspensions containing vacuum freeze dried starch nanoparticles was quite opposite to that of suspensions containing spray dried starch nanoparticles. Hence, we conclude that the application of different drying methods affects the re-depression of starch nanoparticles into water and also impacts on the interactions between starch nanoparticles. Further detailed studies are required to better explain the mechanism of effect of NaCl on the rheological properties of starch nanoparticle suspensions.

Acknowledgements

This research was supported by National Natural Science Foundation of China (31000813), Chinese Universities Scientific Fund (2012QJ009), High Technology Research and Development Program of China (2011AA100802), Commonweal Guild Agricultural Scientific Research Program of China (201003077), and Beijing Municipal Science and Technology Commission Project (D12110003112002).

References

Amiri, A., Øye, G., & Sjöblom, J. (2009). Influence of pH, high salinity and particle concentration on stability and rheological properties of aqueous suspensions of fumed silica. *Colloids and Surfaces A: Physicochemical and Engineering Aspects*, *349*, 43–54.

Barnes, H. A., Hutton, J. F., & Walter, K. (1989). *An introduction to rheology*. Amsterdam: Elsevier., pp. 115–137.

Batrd-Parker, A. C., Boothroyd, M., & Jones, E. (1970). The effect of water activity on the heat resistance of heat sensitive and heat resistant strains of salmonellae. *Journal of Applied Bacteriology*, *33*, 515–522.

Carneiro-da-Cunha, M. G., Cerqueira, M. A., Souza, B. W. S., Teixeira, J. A., & Vicente, A. A. (2011). Influence of concentration, ionicstrength and pH on zeta potential and mean hydrodynamic diameter of edible polysaccharide solutions envisaged for multinanolayered films production. *Carbohydrate Polymers*, *85*(3), 522–528.

Chakraborty, S., Sahoo, B., Teraoka, I., Miller, L. M., & Gross, R. A. (2005). Enzyme-catalyzed regioselective modification of starch nanoparticles. *Macromolecules*, *38*, 61–68.

Cheng, Y.-c., Guo, J.-j., Liu, X.-h., Sun, A.-h., Xu, G.-j., & Cui, P. (2011). Preparation of uniform titania microspheres with good electrorheological performance and their size effect. *Journal of Materials Chemistry*, *21*, 5051–5056.

Chiotelli, E., Pilosio, G., & Le Meste, M. (2002). Effect of sodium chloride on the gelatinization of starch: A multimeasurement study. *Biopolymers*, *63*(1), 41–58.

Chung, C., Degner, B., & McClements, D. J. (2012). Rheology and microstructure of bimodal particulate dispersions: Model for foods containing fat droplets and starch granules. *Food Research International*, *48*, 641–649.

Chung, H.-J., Min, D., Kim, J.-Y., & Lim, S.-T. (2007). Effect of minor addition of Xanthan on Cross-linking of rice starches by dry heating with phosphate salts. *Journal of Applied Polymer Science*, *105*, 2280–2286.

Corcione, C. E., Cavallo, A., Pesce, E., Greco, A., & Maffezzoli, A. (2011). Evaluation of the degree of dispersion of nanofillers by mechanical, rheological, and permeability analysis. *Polymer Engineering and Science*, *51*(7), 1280–1285.

Dendukuri, D., & Doyle, P. S. (2009). The synthesis and assembly of polymeric microparticles using microfluidics. *Advanced Materials*, *21*(41), 4071–4086.

Deng, X.-y., Luan, Q.-x., Chen, W.-t, Wang, Y.-l., Wu, M.-h., Zhang, H.-j., et al. (2009). Nanosized zinc oxide particles induce neural stem cell apoptosis. *Nanotechnology*, *20*(115101), 7.

Jain, A. K., Khar, R. K., Ahmed, F. J., & Diwan, P. V. (2008). Effective insulin delivery using starch nanoparticles as a potential trans-nasal mucoadhesive carrier. *European Journal of Pharmaceutics and Biopharmaceutics*, *69*, 426–435.

Jia, Y., Peng, K., Gong, X.-L., & Zhang, Z. (2011). Creep and recovery of polypropylene/carbon nanotube composites. *International Journal of Plasticity*, *27*(8), 1239–1251.

Katiyar, A., Singh, A. N., Shukla, P., & Nandi, T. (2012). Rheological behavior of magnetic nanofluids containing spherical nanoparticles of Fe–Ni. *Powder Technology*, *224*, 86–89.

Kestin, J., Khalifa, H. E., & Correia, R. J. (1981). Tables of the dynamic and kinematic viscosity of aqueous NaCl solutions in the temperature range 20–150 °C and the pressure range 0.1–35 MPa. *Journal of Physical and Chemical Reference Data*, *10*, 71–88.

Le Corre, D., Bras, J., & Dufresne, A. (2010). Starch nanoparticles: A review. *Biomacromolecules*, *11*, 1139–1153.

Lee, S. J., Choi, S. J., Li, Y., Decker, E. A., & McClements, D. J. (2011). Protein-stabilized nanoemulsions and emulsions: Comparison of physicochemical stability, lipid oxidation, and lipase digestibility. *Journal of Agricultural and Food Chemistry*, *59*, 415–427.

Li, J., & Huang, Q. (2012). Rheological properties of chitosan–tripolyphosphate complexes: From suspensions to microgels. *Carbohydrate Polymers*, *87*(2), 1670–1677.

Lin, N., Huang, J., Chang, P. R., Anderson, D. P., & Yu, J.-h. (2011). Preparation, modification, and application of starch nanocrystals in nanomaterials: A review. *Journal of Nanomaterials*, *20*, 1–13.

Liu, D.-g., Wu, Q.-l., Chen, H.-h., & Chang, P. R. (2009). Transitional properties of starch colloid with particle size reduction from micro to nanometer. *Journal of Colloid and Interface Science*, *339*, 117–124.

Lu, K. (2007). Rheological behavior of carbon nanotube-alumina nanoparticle dispersion systems. *Powder Technology*, *177*, 154–161.

Marcotte, M., Taherian, A. R., Trigui, M., & Ramaswamy, H. S. (2001). Evaluation of rheological properties of selected salt enriched food hydrocolloids. *Journal of Food Engineering*, *48*(2), 157–167.

Mewis, J., & Wagner, N. J. (2009). Current trends in suspension rheology. *Journal of Non-Newtonian Fluid Mechanics*, *157*(3), 147–150.

Nasser, M. S., & James, A. E. (2009). The effect of electrolyte concentration and ph on the flocculation and rheological behaviour of kaolinite suspensions. *Journal of Engineering Science and Technology*, *4*(4), 430–446.

Santander-Ortega, M. J., Stauner, T., Loretz, B., Ortega-Vinuesa, J. L., Bastos-González, D., Wenz, G., et al. (2010). Nanoparticles made from novel starch derivatives for transdermal drug delivery. *Journal of Controlled Release*, *141*(1), 85–92.

Shi, A.-M., Li, D., Wang, L.-J., Li, B.-Z., & Adhikari, B. (2011). Preparation of starch-based nanoparticles through high-pressure homogenization and miniemulsion cross-linking: Influence of various process parameters on particle size and stability. *Carbohydrate Polymers*, *83*(4), 1604–1610.

Shi, A.-m., Li, D., Wang, L.-j., & Adhikari, B. (2012a). The effect of NaCl on the rheological properties of suspension containing spray dried starch nanoparticles. *Carbohydrate Polymers*, *90*(4), 1530–1537.

Shi, A.-m., Li, D., Wang, L.-j., & Adhikari, B. (2012b). Rheological properties of suspensions containing cross-linked starch nanoparticles prepared by spray and vacuum freeze drying methods. *Carbohydrate Polymers*, *90*(4), 1732–1738.

Shi, A.-m., Wang, L.-j., Li, D., & Adhikari, B. (2012). The effect of annealing and cryoprotectants on the properties of vacuum-freeze dried starch nanoparticles. *Carbohydrate Polymers*, *88*(4), 1334–1341.

Shi, A.-m., Li, D., Wang, L.-j., Zhou, Y.-g., & Adhikari, B. (2012). Spray drying of starch submicron particles prepared by high pressure homogenization and miniemulsion cross-linking. *Journal of Food Engineering*, *113*, 399–407.

Simi, C. K., & Emilia Abraham, T. (2007). Hydrophobic grafted and cross-linked starch nanoparticles for drug delivery. *Bioprocess and Biosystems Engineering*, *30*(3), 173–180.

Srivastava, S., Shin, J. H., & Archer, L. A. (2012). Structure and rheology of nanoparticle–polymer suspensions. *Soft Matter*, *8*, 4097–4108.

Susan-Resiga, D., Bica, D., & Vékás, L. (2010). Flow behaviour of extremely bidisperse magnetizable fluids. *Journal of Magnetism and Magnetic Materials*, *322*(20), 3166–3172.

Tabilo-Munizaga, G., & Barbosa-Cánovas, G. V. (2005). Rheology for the food industry. *Journal of Food Engineering*, *67*(1–2), 147–156.

Tian, H.-f., & Xu, G.-z. (2011). Processing and characterization of glycerol-plasticized soy protein plastics reinforced with citric acid-modified starch nanoparticles. *Journal of Polymers and the Environment*, *19*(3), 582–588.

Wang, Y., Wang, L.-J., Li, D., Xue, J., & Mao, Z.-H. (2009). Effects of drying methods on rheological properties of flaxseed gum. *Carbohydrate Polymers*, *78*(2), 213–219.

Wittmar, A., Ruiz-Abad, D., & Ulbricht, M. (2012). Dispersions of silica nanoparticles in ionic liquids investigated with advanced rheology. *Journal of Nanoparticle Research*, *14*, 651.

Xin, X., Xu, G., Wu, D., Li, Y., & Cao, X. (2007). The effect of $CaCl_2$ on the interaction between hydrolyzed polyacrylamide and sodium stearate: Rheological property study. *Colloids and surfaces a: physicochemical and engineering aspects*, *305*, 138–144.

Yin, J.-B., Xia, X., Xiang, L.-Q., Qiao, Y.-P., & Zhao, X.-P. (2009). The electrorheological effect of polyaniline nanofiber, nanoparticle and microparticle suspensions. *Smart Materials and Structures*, *18*(095007), 11.